Ductile deformation in alumina/silicon carbide nanocomposites

DUCTILE DEFORMATION IN ALUMINA/SILICON CARBIDE NANOCOMPOSITES

Houzheng Wu[1] Steve Roberts[2] Brian Derby[3]
[1]Department of Materials, Loughborough University, Leicestershire, LE11 3TU, UK
[2]Department of Materials, Oxford University, Parks Road, Oxford, OX1 3PH, UK
[3]Materials Science Centre, The University of Manchester, Grosvenor Street, Manchester, M1 7HS, UK

ABSTRACT

A transmission electron microscope study on cross sections obtained from ground and polished surfaces has revealed that ductile deformation is dominated by dislocations in alumina/silicon carbide nanocomposites containing 1, 5 and 10 vol% silicon carbide particles, and by twinning in unreinforced alumina. The dispersed silicon carbide particles in alumina/silicon carbide nanocomposites restrict the motion of dislocations. A dislocation pinning model is used to compare the possible mechanisms of deformation in alumina and the nanocomposites. Cr-fluorescence piezospectroscopy has been used to characterise the residual stress levels in the materials studied. The measured broadening of the Al_2O_3/Cr^{3+} fluorescence peak indicates a dislocation density of 7.3 - 9.7 x 10^{16} m^{-2} under the indentations in the nanocomposites, whilst the beneath indentations in alumina is 1-2 orders of magnitude smaller.

INTRODUCTION

It has been nearly two decades since Niihara and Nakahira reported significant improvements in bend strength, up to about 300%, of polycrystalline alumina, and also in fracture toughness, by the addition of 5-10% silicon carbide particles with size < 10^{-6} m[1,2]. These were termed “ceramic nanocomposites”, and a range of nanocomposites have been investigated with different ceramics chosen as the matrix and particles of various compounds or metals as dispersants. Among these nanocomposites, the most studied have been those with matrices of alumina polycrystals containing silicon carbide particles as the dispersants. A number of different studies have attempted to validate the claimed improvements in mechanical properties of alumina/silicon carbide nanocomposites, as well as to explore any other characteristics of the nanocomposite structure[3,4,5,6,7,8,9,10,11,12].

Large variations have been reported in the flexural strength and fracture toughness values reported by different workers, and it is now generally agreed that the improvement in bend strength is modest at best, and improvements in fracture toughness are negligible. It appears that the bend strength is largely influenced by the processing factors, rather the nanostructure alone[13,14], and apparent fracture toughness and bend strength improvements can be largely attributed to residual surface compressive stresses in the nanocomposites due to their different response to grinding and polishing than is found with monolithic polycrystalline alumina[3,12].

A transition of fracture mode, in bending or in surface grinding, from intergranular in monolithic alumina to transgranular in the nanocomposites has been consistently found. This genuine “nanocomposite effect” has been observed in nanocomposites where the SiC particle content is as low as 1 vol%, and in materials produced by either hot-pressing or pressureless sintering[10,11]. Further, several studies have noted that it is easier to produce a fine polished surface with the nanocomposites than is achievable with alumina[10,11]. This is believed to be related to the decreased incidence of grain-boundary fracture and grain pull-out in the nanocomposite [15]. The wear resistance of the nanocomposites is generally increased by a factor of 3 to 5 over alumina with similar grain size; this improvement is observed in both erosion and in sliding wear[9,16]. The ease of polishing and the superior wear resistance indicates that contact damage in the near surface region of the nanocomposites is somewhat different from that found in alumina.

Our earlier experimental studies[12] indicated that ductile deformation caused by contact damage plays a key role in the behaviour of alumina/silicon carbide nanocomposites. In this paper, we report complementary analyses of sub-surface deformation in ground alumina/silicon carbide nanocomposites and monolithic alumina ceramics of similar grain size by cross-sectional TEM and Cr-fluorescence spectroscopy measurements.

EXPERIMENTAL DETAILS AND ANALYSIS TECHNIQUE

Full details of the methods of preparation and manufacture of the materials have been set out in detail elsewhere[12] but a brief description follows. Samples of alumina/silicon carbide nanocomposites were fabricated by hot pressing in a graphite die at 1650 to 1680 °C for 1 hr under a pressure of 20 - 25 MPa under flowing argon. The nanocomposite consisted of an alumina matrix material containing 1-10% by volume submicron SiC particles. Alumina powder, with submicron particle size (AKP53: Sumitomo, Tokyo, Japan), was used as the matrix. The SiC particles were a commercial α-SiC powder (UF 45: Lonza - now H. C. Starck, Goslar, Germany), with a mean particle size of ~90 nm. The hot pressed discs were ground to remove the top surface on both sides with an epoxy resin bonded diamond wheel (grit size 150 μm) to achieve a specimen thickness of about 3 mm. A wheel speed of 1250 rpm, table translation speed of 0.8 ms^{-1} and feed depth of 12.5 μm per pass was used in this process. Specimens with polished surfaces were produced by lapping successively with 25, 8, 3 and 1 μm diamond slurry on a Kent III polishing machine (Kemet International, Maidstone, UK) with Lamplan plates (Kemet International) rotating at about 60 rpm and with an external load of 15 N.

Cross section TEM samples with ground or polished surfaces were made by ion-milling[12]. The TEM observations were carried out in JEOL200CX and JEOL4000 miscroscopes.

A microindenter (Matsuzawa MHT-2, Japan) was used to produce indents on 1 μm – polished surfaces of alumina and alumina / silicon carbide nanocomposites, using a Vickers diamond indenter tip. The load range used was 500g and 1000g, with a hold time of 15 seconds.

Fluorescence spectra were acquired using a Raman microprobe system (Renishaw, Wotton-under-Edge, UK) using a He-Ne (632.8 nm) laser with a beam intensity of about 1.0 mW. Measurements were made using a × 40 microscope objective lens with a numerical aperture of 0.65, giving an approximate beam diameter on the specimen of 2 μm. To minimise any peak shift due to temperature fluctuations, all calibrations and tests were performed in a temperature-controlled room; to eliminate any remaining temperature-induced changes, a characteristic neon line at 14431 cm^{-1} was used as a frequency standard; full operational details are given in a previous publication[17].

The collected data were subsequently analysed with curve-fitting algorithms included in the SpectraCalc software package (Galactic Industries Corp., Salem, NH, USA). The line position and width were identified by simultaneously fitting the R1 and R2 fluorescence peaks with combined Gaussian / Lorentz function. Repetitions of measurements on the same location showed that the standard deviation between such measurements is small enough to be ignored. For all probe positions, therefore, only one measurement was made.

THE INFLUENCE OF SIC PARTICLES ON DUCTILE DEFORMATION IN ALUMINA

The possible slip systems in Al_2O_3 crystal are summarised by Snow and Heuer[18]. The self-energy of a dislocation is proportional to the square of its Burgers' vector (b^2); the magnitudes of the possible Burgers vectors are in the following order:

$$b_{1/3\langle 11\bar{2}0\rangle} < b_{1/3\langle \bar{1}101\rangle} < b_{1/3\langle \bar{1}021\rangle} < b_{\langle 10\bar{1}0\rangle} < b_{1/3\langle 21\bar{3}1\rangle} < b_{1/3\langle \bar{1}012\rangle}$$

Among these, basal slip is expected to have the lowest critical resolved shear stress.

Two kinds of twin have been confirmed to operate in the plastic deformation of alumina: basal twins and rhombohedral twins. Their crystallographic elements were unambiguously determined as following:

Basal twin:

$K_1 = (0001)$ $\eta_1 = <10\bar{1}0>$ $K_2 = \{10\bar{1}1\}$ $\eta_2 = <\bar{1}012>$ $s = 0.635$

Rhombohedral twin:

$K_1 = (10\bar{1}2)$ $\eta_1 = <\bar{1}012>$ $K_2 = (\bar{1}012)$ $\eta_2 = <10\bar{1}1>$ $s = 0.202$

where K_1 is the twinning plane, η_1 the twinning direction, K_2 the reciprocal twinning plane, η_2 the reciprocal twinning direction, and s the deformation shear. For the twinning process, Kronberg[19] suggested a complicated synchronous movement of quarter-partial dislocations with $1/3<11\bar{2}0>$ Burgers vectors. This mechanism involves the shear of an oxygen layer by a $1/3<11\bar{2}0>$ quarter-partial, followed by an additional shear of the adjoining aluminium layer by a $1/3<2\bar{1}\bar{1}0>$ quarter partial. The repetition of this sequence of alternate motions on successive planes gives the correct structure for the sheared proportion.

Geipel *et al*[20] described the rhombohedral twinning process in terms of a cross-slip twinning model involving dissociated dislocations. The perfect $^1/_3<0\bar{1}11>$ dislocation is imagined to dissociate into a leading partial with Burgers vector of $^1/_{21.9}<0\bar{1}11>$ and a trailing partial with a Burgers vector of $(^1/_3-^1/_{29.5})<0\bar{1}11>$. Under applied stress, the leading partial will glide to form faulted loops and approach the trailing partial from behind, and then recombine on $(01\bar{1}2)$ plane. By the forced cross slip of $^1/_3<0\bar{1}11>$, the dislocation will dissociate again and form another faulted loop. The continuation of this process leads to the formation of a rhombohedral twin.

It has been demonstrated that all of the main slip systems can be activated under tensile or hydrostatic compression loading at temperatures above the brittle-ductile transition temperature of Al_2O_3, (> ~1100 °C) [21]. Twinning, as a special type of slip, was also observed under uniaxial compression at this temperature regime[22].

At temperatures below the brittle-ductile transition temperature, plastic deformation is difficult, and more complex, varying strongly with loading condition. Dislocation slip is in general activated under hydrostatic compression conditions with significant shear components[23]. Sharp point indentation, scratching, and abrasion, produces such conditions. Twins have been widely found in single or polycrystalline alumina under loading conditions such as grinding or polishing, sliding wearing, indentation or scratch, bending tests, uniaxial or hydrostatic compression, and thermal down-shock. Basal twins have been much more frequently observed than rhombohedral twins in all these cases. The thickness of the twins was found to be smaller than a few μm for basal twins and frequently down to tens of nanometres, and for rhombohedral twins, ranged from about 1 μm to about 50 μm. Resolved shear stresses for twinning were measured as 12.6 MPa between 627°C and 1100°C, and 227 MPa at 350°C[24].

When SiC particles are dispersed inside the alumina grains, these particles can act obstacles to dislocation motion and to twin growth. As twinning can be considered as caused by a specific type of slip processes, we simplify the problem here and only consider basal slip in the following analysis.

Assume the SiC particles are single-sized spheres with a radius of $2r$, and dispersed in an alumina matrix in a simple cubic lattice with a lattice spacing ($2r + L$), as shown in fig. 1(a), where each SiC particle occupies one lattice point. The gap between two particles, L, has the following relationship with the radius of SiC particles (r) and the volume fraction (f):

$$L = \left[\left(\frac{4\pi}{3f}\right)^{1/3} - 2\right] r \qquad (1)$$

In order to bypass SiC particles, dislocation lines assume a curved shape; the maximum shear stress needed to bow a dislocation segment into a circular arc is given by the following equation[25]

$$\Delta\tau = \frac{\mu b}{L}\cos\left(\frac{\phi_c}{2}\right) \tag{2}$$

where ϕ_c is critical angle for the obstacle to be by-passed by a dislocation, μ is the shear modulus of alumina, and b is the Burgers' vector. For alumina, G = 150 GPa, and for basal slip $b_{1/3<2\bar{1}\bar{1}0>}$ = 0.476 nm. The maximum critical shear stress, taking ϕ_c = 0 (appropriate for hard, impenetrable obstacles), for a dislocation to by-pass the SiC particles is thus:

$$\Delta\tau = \frac{71.4 f^{1/3}}{(1.6 - 2f^{1/3})r} \text{ (GPa)} \tag{3}$$

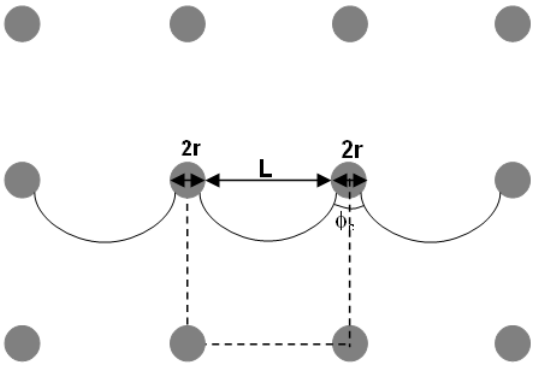

a)

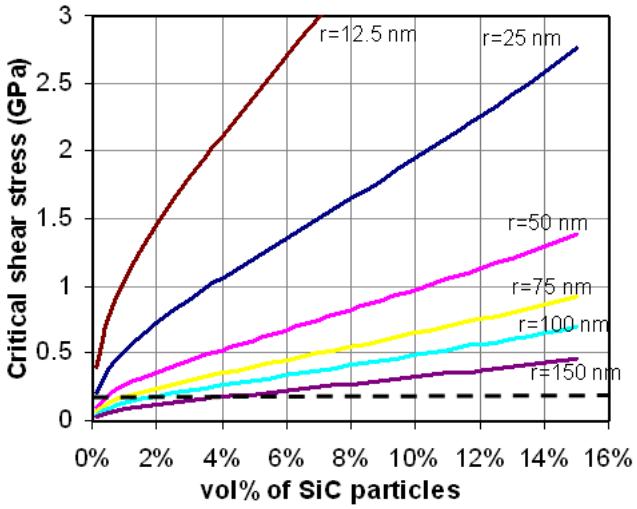

b)

Fig. 1 The effect of SiC particles on the obstacle of dislocation motion in alumina. (a) a simple cubic lattice arrangement of SiC particle with 2r as the diameter of the particles, L the shortest gap between two particles, ϕ_c the critical angle for dislocations to by-pass the particles under an increasing stress. (b) critical resolved shear stress versus the particle size and volume percent, for dislocations to by-pass the particles in alumina/silicon carbide nanocomposites

The modelling results shown in Fig. 1(b) indicates that as little as about 1 vol% SiC particles with a diameter smaller than 150 nm can generate a dislocation motion resistance that is larger than the measured critical shear stress for basal twinning in alumina, 227 MPa at 350°C (represented by the dashed line in fig. 1(b)). For smaller particle sizes, the resistance to dislocation motion increases more rapidly with the increasing volume fraction.

EXPERIMENTAL RESULTS AND DISCUSSION

(a) Ductile Deformation Observed by TEM

For surfaces polished with 1, 3 or 8 μm diamond grits, the deformation induced was dominated by dislocations, as shown in fig. 2. The dislocations were observed to by-pass the SiC particles by

bowing, as indicated by arrows. Fig. 1(b) indicates that the level of the resistance dislocation motion for hard particles of this size and spacing is under 1 GPa (particles size >100 nm up to 10 vol %). Compared to the expected level of shear stress around a sharp indenter[26], this level of resistance is not significant; this correlates well with the TEM-based observation that the depths of the dislocated regions underneath the polished surfaces of the nanocomposites and the alumina were very similar at 0.3-1.5 μm[17].

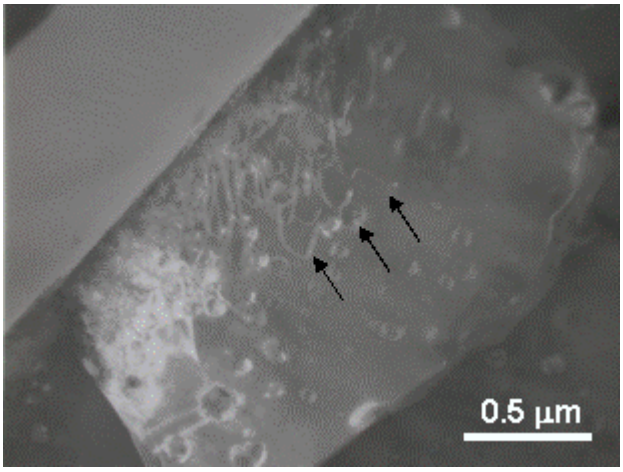

a)

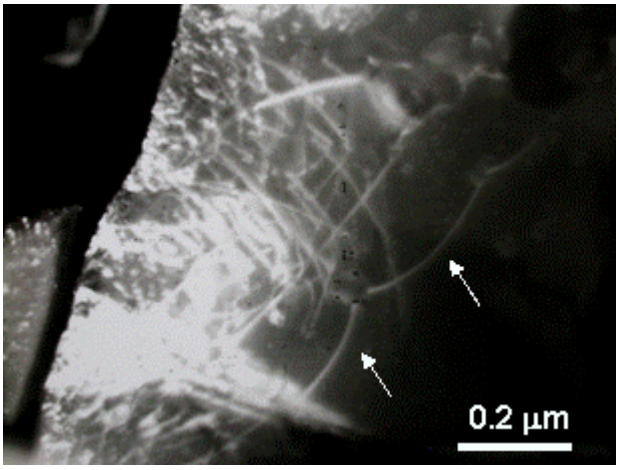

b)

Fig. 2 Cross-section views of the grains underneath polished surfaces of Al_2O_3/SiC nanocomposites. Only dislocations were generated with no twins observed. Dislocations bow around SiC particles, as arrowed.

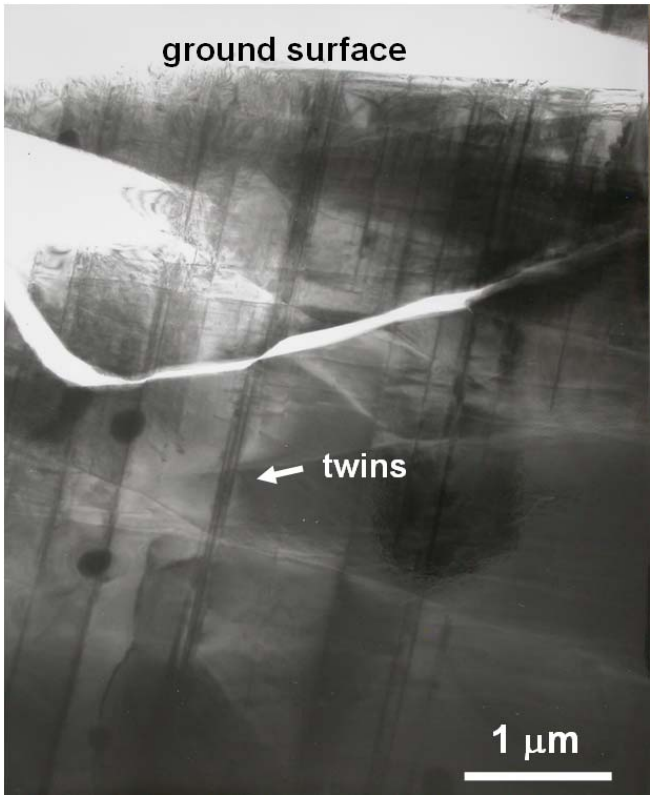

a)

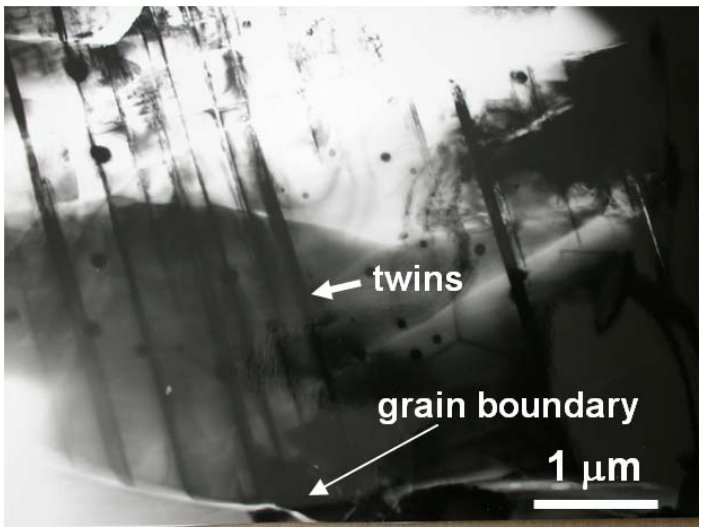

b)

Fig. 3 Cross-section views of ductile deformation beneath the ground surface of polycrystalline alumina. (a) near-surface; (b) near a sub-surface grain boundary.

TEM examination of cross-sections of ground surfaces of unreinforced alumina shows that the ductile deformation is dominated by twins (see Fig. 3). Electron diffraction pattern confirms that these twins are basal twins. The twins initiated on the ground surface, and then grew through the whole grain until meeting the grain boundary; close to the ground surface, dislocations also form, as shown in fig. 3(a), though they do not penetrate as deeply as the basal twins. This confirms that, in pure alumina at low temperatures, twins are easy to generate; the critical shear stress is reported to be ~ 200 MPa at 350 °C[24]. The local temperature during grinding of the ceramic surface is unknown but will be lower than the ductile brittle transition (~1100 °C).

Underneath the ground surfaces of the nanocomposites dislocations dominate, as shown in fig. 4; only occasionally were twins noticed in some grains, but in very low density, as shown in fig. 5. As was found beneath the polished surfaces, high dislocation densities were found either in the deformed surface grains or in grains underneath them up to a depth of 3-10 μm (see previous publication[12]). When twins were developed in a grain of the nanocomposites, their number was significantly reduced, compared to alumina. In fig. 5, only two twins were developed, and the rest of the grain was occupied by dislocations; these twins have by-passed a SiC particle, and become tapered thereafter (see fig. 4(b)). However, neither twin has reached the grain boundary. It is possible that the growth of the twins may have been restricted by the SiC particles in this grain. This implies that the SiC particles impede the propagation of twins in the nanocomposites.

The model predictions in fig 1(b) show that, in alumina dispersed with 5vol% silicon carbide particles of 100 nm diameter, the resistance for the motion of basal dislocations is about 600 MPa, and higher than the required critical shear stress, 225 MPa, for basal twins. The fact that there are few basal twins on the ground surface of Al_2O_3/ 5vol%SiC nanocomposite implies that the simple model is valid, as a first approximation. Accordingly, we hypothesise that, when the resistance generated by the dispersed particles is higher than the required critical shear stress of twins, the growth of twins could be significantly constrained. If this hypotheses is valid, 1vol% of SiC particle could be sufficient to constrain the twinning mechanism in alumina, because the calculated resistance (260MPa), using equation (2), is larger than reported critical shear stress.

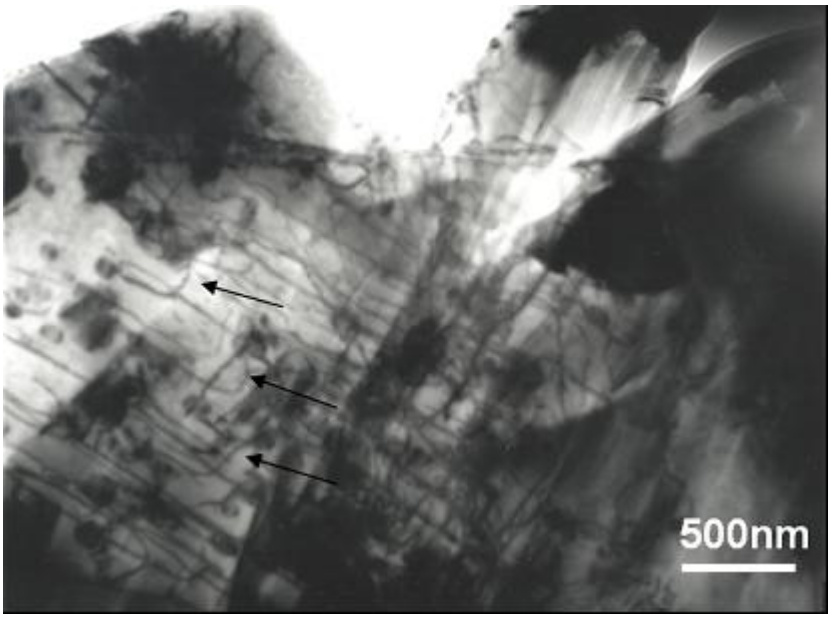

Fig. 4 Cross-section view of ductile deformation beneath a ground surface of Al_2O_3/SiC nanocomposite. Note the bowing of dislocation lines between SiC particles, as arrowed.

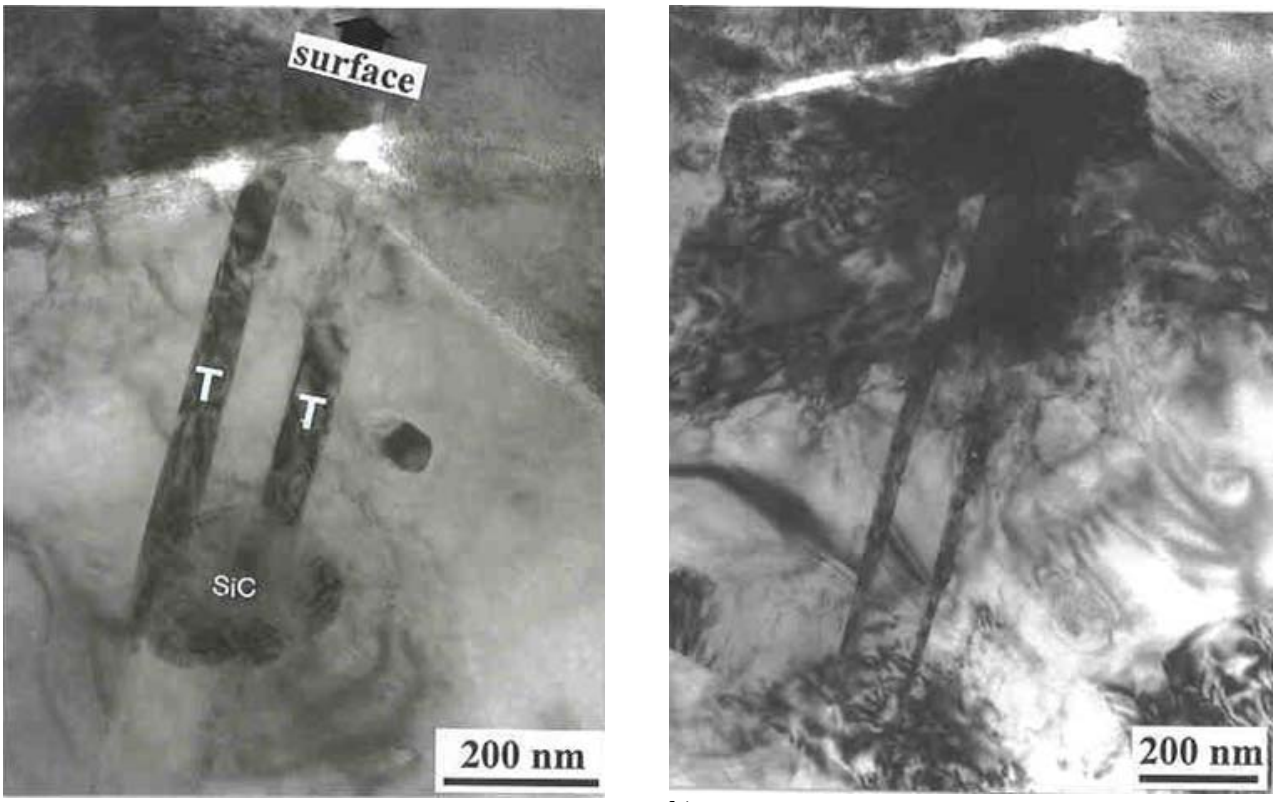

a) b)

Fig. 5 Cross section view of grains beneath a ground surface of Al_2O_3/SiC nanocomposite. Two twins were initiated at a grain boundary; (a) a SiC particle blocks one of the twins; (b) two twins become thinner on passing a SiC particle.

(b) Dislocation Density

It was not possible to characterize the dislocations, due to the high strains arising from the high dislocation density and from thermal misfit between the alumina matrix and SiC particles. Similarly it was not possible to quantify the dislocation density from TEM images. Hence the broadening of Al_2O_3/Cr^{3+} fluorescence lines was used to estimate the dislocation densities. Details of the methodology are given elsewhere[17].

Sharp indenters, like Vickers indenter, have been used to simulate the grinding process; it is generally agreed that there are similarities in fracture and ductile deformation between the machined ceramics surfaces and the indented surfaces using sharp indenters. Information on the ductile deformation in indents can reflect what could happen on the machined surfaces. By using the measured maximum values of full width at half maximum (FWHM) of the fluorescence peak inside the Vickers indents, we can plot the dislocation density vs the content of SiC particles dispersed inside the nanocomposites, as shown in fig. 6. In this chart, the measurements included those for indents created under different normal loads, i.e. 5 N and 10 N. Under the same indenting load, the nanocomposites have a higher dislocation density than alumina, with a difference of about 1-2 orders of magnitude. This difference echoes the observed difference in the ductile region on the ground surfaces of alumina and the nanocomposites.

These results also firmly demonstrate that there is little difference in dislocation density in the nanocomposites dispersed with different SiC contents. It seems that a dispersion of 1 vol% SiC is enough to have a different ductile deformation in alumina. This ductile deformation should be

dominated by dislocations, unlikely to be twinning, otherwise the dislocation density should not be the same as those measurements on the nanocomposites with 5 and 10 vol% SiC particles.

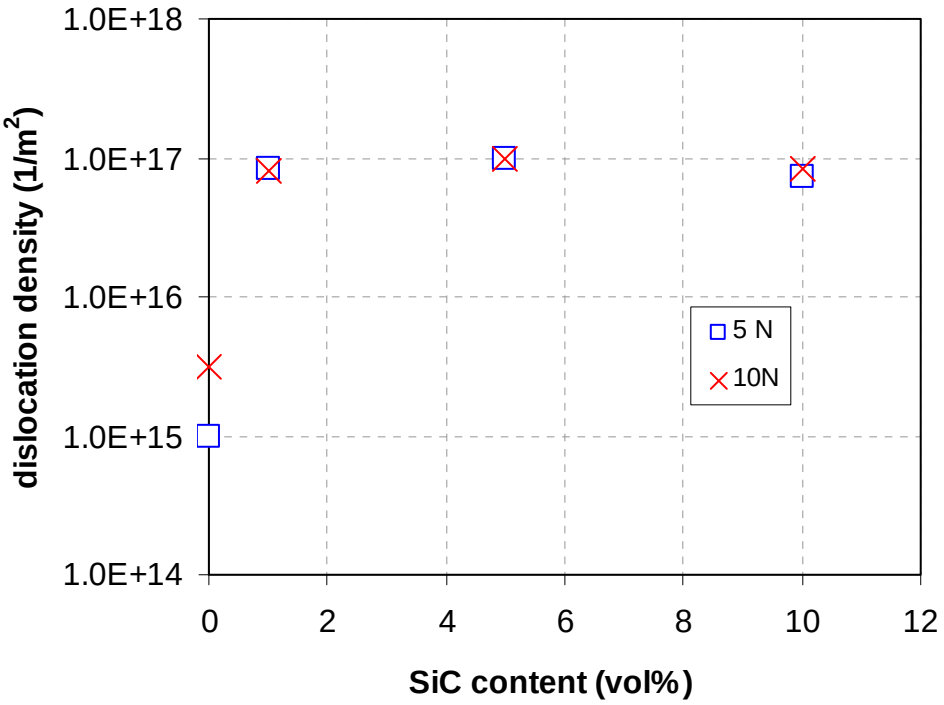

Fig. 6 Dislocation density underneath the indents of Al_2O_3 and Al_2O_3/SiC nanocomposites with different vol% of SiC dispersants. The indents were created with Vickers indenter with a normal load of 5N and 10N.

SUMMARY

Cross sectional TEM examination of the ground and polished surfaces shows that SiC particles dispersed in alumina matrix are likely becoming obstacles to dislocation motion. When the particle sizes are in submicron range, the resistance for dislocations in alumina to by-pass the SiC particles is less than 1 GPa, which is too small, comparing to the shear stress around a sharp indenter, to significantly influence the size of dislocation activating region underneath the machined surfaces or indents. However, it was this resistance that is high enough to constrain the development and growth of basal twins. The modelling prediction and the estimated dislocation density both support that only 1 vol% silicon carbide particles in a size of ~100 nm in diameter used in this study, is enough to constrain the twinning. The estimated dislocation density in Vickers indents using the broadening of fluorescence line is 1-2 orders less in alumina than in the nanocomposites; among the nanocomposites, the dislocation density is the same, between 7.3 to 9.7 x $10^{16}/m^2$, for a silicon carbide reinforcements content of 1, 5 and 10vol%.

REFERENCES

[1] K. Niihara & A. Nakahira: Strengthening of Oxide Ceramics by SiC and Si_3N_4 Dispersions, *Proc. 3rd Int. Symp. on Ceramic Materials and Components for Engines*, edt. by V.J. Tennery. The Am. Ceram. Soc., Westerville, Ohio, pp 919-926 (1988).

[2] K. Niihara: New Design Concept of Structural Ceramics-Ceramics Nanocomposites, The Centennial Issue of the Ceramic Society of Japan, *J. Ceram. Soc. Jpn*, **99**, 974-82 (1991).

[3] J. Zhao, L.C. Stearns, M.P. Harmer, H.M. Chan, G.A. Miller & R.F. Cook: Mechanical Behaviour of Alumina-Silicon Carbide "Nanocomposites", *J. Am. Ceram. Soc.*, **76**[2], 503-510 (1993).

[4] T. Ohji, A. Nakahira, T. Hirano & K. Niihara: Tensile Creep-behaviour of Alumina Silicon-Carbide Nanocomposite, *J. Am. Ceram. Soc.*, **77**[12], 3259-3262 (1994).

[5] R.W. Davidge, R.J. Brook, F. Cambier, M. Poorteman, A. Leriche, D. O'Sullivan, S. Hampshire & T. Kennedy: Fabrication, Properties, and Modelling of Engineering Ceramics Reinforced with Nanoparticles of Silicon Carbide, *Brit. Ceram. Trans.*, **96**, 121-127 (1997).

[6] S. Maensiri & S.G. Roberts: Thermal Shock Resistance of Sintered Alumina/Silicon Carbide Nanocomposites Evaluated by Indentation Techniques, *J. Am. Ceram. Soc*, **85**[8], 1971-1978 (2002).

[7] C.N. Walker, C.E. Borsa, R.I. Todd, R.W. Davidge & R.J. Brook: Fabrication, Characterisation and Properties of Alumina Matrix Nanocomposites, *Br. Ceram. Proc.*, **53**, 249-264 (1994).

[8] M. Sternitzke, E. Dupas, P. Twigg & B. Derby: Surface Mechanical Properties of Alumina Matrix Nanocomposites, *Acta Mater.*, **45**[10], 3963-3973 (1997).

[9] J. Rodriguez, A. Martin, J.Y. Pastor, J. Llorca, J.F. Bartolome & J.S. Moya: Sliding Wear of Alumina/Silicon Carbide Nanocomposites, *J. Am. Ceram. Soc.*, **82**[8], 2252-2254 (1999).

[10] A.J. Winn & R.I. Todd: Microstructural Requirements for Alumina-SiC Nanocomposites , *Brit. Ceram. Trans*, **98**[5], 219-224 (1999).

[11] H. Kara & S.G. Roberts: Polishing Behavior and Surface Quality of Alumina and Alumina/Silicon Carbide Nanocomposites, *J. Am. Ceram. Soc.*, **83**[5], 1219-1225 (2000).

[12] H.Z. Wu, C.W. Lawrence, S.G. Roberts & B. Derby: The Strength of Al_2O_3/SiC Nanocomposites after Grinding and Annealing, *Acta Mater.*, **46**[11], 3839-3848 (1998).

[13] J. Perez-Rigueiro, J.Y. Pastor, J. Llorca, M. Ellices, P. Miranzo & J.S. Moya: Revisiting the Mechanical Behavior of Alumina Silicon Carbide Nanocomposites, *Acta Mater.* **46**[15], 5399-5411 (1998).

[14] L. Carroll, M. Sternotzke & B. Derby: Silicon Carbide Particle Size Effects in Alumina-based Nanocomposites, *Acta Mater.* **44**[11], 4543-4552 (1996).

[15]J.L. Ortiz-Merino & R.I. Todd: Relationship Between Wear Rate, Surface Pullout and Microstructure During Abrasive Wear of Alumina and Alumina/SiC Nanocomposites, *Acta Mater.* **53**[12], 3345-3357 (2005).

[16] H.J. Chen, W.M. Rainforth & W.E. Lee: The Wear Behaviour of Al_2O_3-SiC Ceramic Nanocomposites, *Script Mater.*, **42**[8], 555-560 (2000).

[17] H.Z. Wu, S.G. Roberts & B. Derby: Residual Stress Distributions Around Indentations and Scratches in Polycrystalline Al_2O_3 and Al_2O_3/SiC Nanocomposites Measured Using Fluorescence Probes, *Acta Mater.* **56**[1], 140-149 (2008).

[18] J.D. Snow & A.H. Heuer, Slip Systems in Al_2O_3, *J. Am. Ceram. Soc.*, **56**[3], 153-157 (1973).

[19] M.L. Kronberg: Plastic Deformation of Single Crystals of Sapphire – Basal Slip and Twinning, *Acta Metall.***5**[9], 507-524 (1957).

[20] T. Geipel, K.P.D. Lagerlof, P. Pirouz & A.H. Heuer: A Zonal Dislocation Mechanism for Rhombohedral Twinning in Sapphire (α-Al_2O_3), *Acta Metall. Mater.*, **42**[4], 1367-1372 (1994).

21 J.B. Watchman Jr & L.H. Maxwell: Plastic Deformation of Ceramic-Oxide Single Crystals *J. Am. Ceram. Soc.* **37**[7]**,** 291-299 (1954).

[22] H. Conrad: Mechanical Behaviour of Sapphire, *J. Am. Ceram. Soc.*, **48**[4], 195 (1965).

[23] H.M. Chan & B.R. Lawn: Indentation Deformation and Fracture of Sapphire *J. Am. Ceram. Soc.*, **71**[1], 29-35 (1988).

[24] W.D. Scott & K.K. Orr: Rohmbohedral Twinning in Alumina, *J. Am. Ceram. Soc.*, **66**[1], 27-32 (1983).

[25] D.J. Green, An Introduction to the Mechanical Properties of Ceramics, Cambridge University Press, pp183 (1998).

[26] E.H. Yoffe: Elastic Stress Fields Caused by Indenting Brittle Materials, *Phil. Mag.* **A 46**[4], 617-628 (1982).